

Supplement of Atmos. Chem. Phys., 18, 11375–11388, 2018  
<https://doi.org/10.5194/acp-18-11375-2018-supplement>  
© Author(s) 2018. This work is distributed under  
the Creative Commons Attribution 4.0 License.



*Supplement of*

## **Transport of Canadian forest fire smoke over the UK as observed by lidar**

**Geraint Vaughan et al.**

*Correspondence to:* Geraint Vaughan ([geraint.vaughan@manchester.ac.uk](mailto:geraint.vaughan@manchester.ac.uk))

The copyright of individual parts of the supplement might differ from the CC BY 4.0 License.

# 1 Capel Dewi Raman LIDAR

The Capel Dewi Raman lidar is a biaxial ultraviolet lidar based on that used for the EARLINET project in 1999–2002 [Wandinger et al., 2004]. Since then, it has been updated and now contains a Continuum 8030 Nd-YAG laser emitting pulses at 354.7 nm at 30 Hz with pulse energy 300 mJ. A tenfold beam-expanding telescope directs the light vertically into the atmosphere. The receiver is based on a 1 m diameter mirror used in a Nasmyth-Cassegrain configuration, which directs the backscattered radiation through a collimator on to a dichroic beamsplitter (Fig. S1). This beamsplitter reflects and transmits radiation with wavelength greater or less than 397 nm, respectively, into the receiver channels. Interference filters centred around 387 and 408 nm isolate Raman scattering from nitrogen and water vapour respectively (Table 1). A third channel measures elastic backscattered radiation reflected from the other two filters. The receiver is mainly sensitive to the polarisation component parallel to the laser, which reduces background noise in the Raman channels but does not permit measurements of the aerosol backscatter when there is a significant cross-polarised component.

The lidar is designed for free tropospheric measurements and so the receiver field-of-view does not fully overlap the laser beam below 2 km. Measurements below 2 km are therefore not used here.

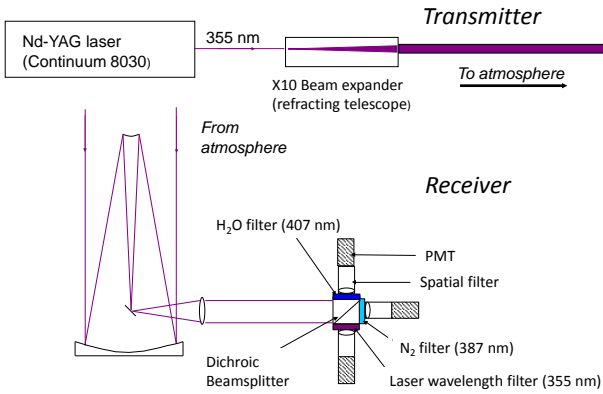


Figure S1: Schematic diagram of the Capel Dewi Raman lidar

Channel	Centre Wavelength nm	Bandwidth FWHM nm	Measured Wavelength $\lambda_m$ , nm	Transmission at $\lambda_m$ , %
H <sub>2</sub> O	408	1.7	407.5	22
N <sub>2</sub>	387	2.6	386.7	22
Elastic	355	5.0	354.7	60

Table 1: Interference filter characteristics for Capel Dewi lidar (FWHM is full width half maximum). Blocking on the Raman filters at 354.7 nm is  $10^{-8}$ . Neutral density filters are used in the elastic channel to avoid saturating the signal at low altitude.

The signals are measured using EMI 9124 photomultipliers and a photon-counting electronics system (ORTEC PCI-MCS) with range resolution 15 m (100 ns time bins). A dead time of 10 ns is applied in the counting system, and corrected accord-

ing to the non-paralysable equation:

$$S = \frac{S_0}{1 - \tau * S_0} \quad (1)$$

where  $S_0$  is the measured count rate,  $S$  is the corrected count rate and  $\tau$  the dead time.

Although elastic measurements can be made in daytime, the Raman signals are too noisy in daytime and are only collected at night. The system is normally operated alongside a second lidar which measures both polarisation components of the elastic signal, but this system was inoperative during the period of interest here.

Measurements were made with the Capel Dewi lidar on the nights of 23–24, 24–25, 26–27, 29–30 and 30–31 May; persistent low cloud cover precluded measurements during the other nights.

## 2 Met Office Raman lidar

The Met Office has established an operational network of Raymetrics Raman and depolarisation lidars around the UK. These are used alongside ceilometers, airborne in situ and remote-sensing observations, satellite retrievals and dispersion model output for volcanic ash monitoring by the London Volcanic Ash Advisory Centre (VAAC) [Marenco et al., 2016]. Like the Capel Dewi lidar, these Raman lidars use the third harmonic of a Nd-YAG laser (Quantel CFR200) at 355 nm. The lasers provide a pulse energy of 50 mJ at 20 Hz, directed vertically via a beam expander to assure eye-safety. The receiving telescopes are 30 cm in diameter with complete overlap achieved around 250 m altitude [Adam et al., 2016]. The range resolution of the receiver is 15 m. Unlike the Capel Dewi lidar, these lidars measure both parallel- and perpendicularly-polarised returns from the atmosphere and therefore provide measurements of aerosol backscatter, depolarisation and lidar ratio as well as optical depth. The method used to calibrate the depolarisation, along with a layout of the receiving unit, is based on that of Freudenthaler et al. [2009].

The lidar has both analogue and photon-counting detection channels, although in this paper only the photon-counting measurements are used. A deadtime correction as above with  $\tau=3.8$  ns is applied to these data. As with the Capel Dewi lidar, Raman measurements can only be used at night, which for the episode considered here (at the end of May in the UK) meant 2100–0300 UTC. The lidars were operated in one of two modes: intermittently for periods of 1 hour every 3 hours, or continuously, but not all of them were operational at any given time (See Table 1 in the main paper).

## 3 Met Office Ceilometers

The Met Office operate an extensive network of ceilometers around the UK, of various types. The 12 Lufft CHM 15k ceilometers are of particular interest to this study, because of their greater sensitivity to thin aerosol layers with low backscatter. These ceilometers emit infrared radiation (1064 nm) and use photon-counting detectors. While they cannot provide the quantitative detail of the Raman lidars, they operate continuously and can provide more complete coverage in space and time of the free-tropospheric aerosol.

## 4 Retrieval method

The power received by a lidar,  $P(z)$ , obeys the lidar equation [Wandinger, 2005], which for elastic ( $P_e$ ) and Raman ( $P_R$ ) scattering takes the form:

$$P_e(z) \propto [\beta_{aer}(z) + \beta_{ray}(z)] \exp[-2 \int_0^z (\sigma_{ray} n(z) + \alpha(z)) dz] \quad (2)$$

and

$$P_R(z) \propto \beta_{ram}(z) \exp[-\int_0^z ((\sigma_{ram} + \sigma_{ray}) n(z) + 2\alpha(z)) dz] \quad (3)$$

respectively. Here,  $\beta_{aer}$ ,  $\beta_{ray}$  and  $\beta_{ram}$  are the backscatter coefficients for aerosol, elastic molecular (Rayleigh) and Raman scattering respectively,  $n(z)$  is the number density of air molecules,  $z$  is the height above the lidar, and  $\sigma_{ram}$  and  $\sigma_{ray}$  are the scattering cross-sections for Raman and Rayleigh scattering by air molecules, which are taken to be  $1.929 \times 10^{-30} \text{ m}^2$  and  $2.76 \times 10^{-30} \text{ m}^2$  respectively [Bates, 1984]. The extinction coefficient of aerosol,  $\alpha$ , is assumed to be the same at the elastic and Raman wavelengths.

## 5 SEVIRI observations on 22-23 May 2016

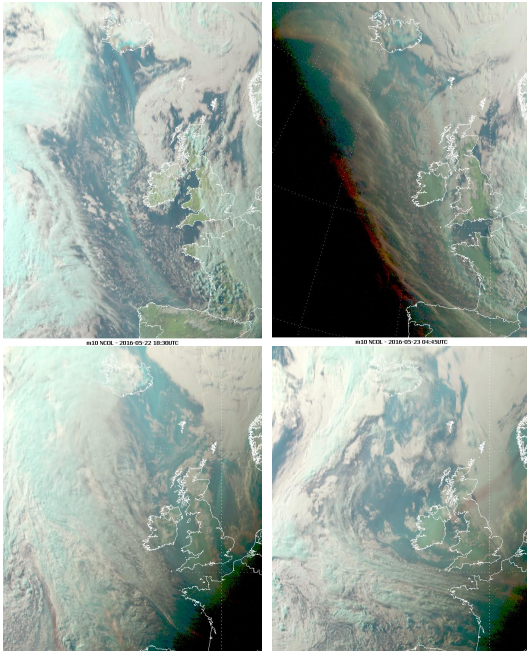


Figure S2: SEVIRI Day Natural Colour RGB images from 1830 UTC 22 May (top left); 0445 UTC 23 May, top right; 1945 UTC 23 May, bottom left; and 1930 UTC 24 May (bottom right). Smoke appears as faint blue-grey streaks. The red-brown streak in the North Sea shown in the bottom right image is the shadow of a smoke streak on some low-lying water clouds. Images taken from EUMETSAT web site.

The EUMETSAT Natural Colour RGB analysis of SEVIRI data shows the arrival of smoke over the UK (Fig. S2). At 1830 UTC on 22 May, a ribbon of smoke extended from northern Spain to Iceland, passing west of Ireland. By 0445 UTC

on the 23rd, this ribbon lay along the Irish Sea, just passing over Camborne at the western tip of Cornwall (consistent with the ceilometer evidence). By 1945 UTC on the 23rd, smoke covered most of the west of the UK and Ireland, and shows a similar pattern 24 hours later.

## References

- Adam, M., Turp, M., Horseman, A., Ordóñez, C., Buxmann, J., & Sugier, J. (2016). From operational ceilometer network to operational lidar network. In B. Gross, F. Moshary, & M. Arend (Eds.), *EPJ Web of Conferences*, volume 119 (pp. 27007).
- Bates, D. (1984). Rayleigh scattering by air. *Planet. Space Sci.*, 32(6), 785–790.
- Freudenthaler, V., Esselborn, M., Wiegner, M., Heese, B., Tesche, M., Ansmann, A., Müller, D., Althausen, D., Wirth, M., Fix, A., Ehret, G., Knippertz, P., Toledano, C., Gasteiger, J., Garhammer, M., & Seefeldner, M. (2009). Depolarization ratio profiling at several wavelengths in pure Saharan dust during SAMUM 2006. *Tellus B*, 61(1), 165–179.
- Marengo, F., Kent, J., Adam, M., Buxmann, J., P., F., & J., H. (2016). Remote sensing of volcanic ash at the Met Office. In B. Gross, F. Moshary, & M. Arend (Eds.), *EPJ Web of Conferences*, volume 119 (pp. 07003).
- Wandinger, U. (2005). Introduction to lidar. In C. Weitkamp (Ed.), *Lidar: Range-Resolved Optical Remote Sensing of the Atmosphere* chapter 1, (pp. 1–18). Springer.
- Wandinger, U., Mattis, I., Tesche, M., Ansmann, A., Bösenberg, J., Chaikowski, A., Freudenthaler, V., Komguem, L., Matthias, V., Pelon, J., Sauvage, L., Sobolewski, P., Vaughan, G., & Wiegner, M. (2004). Air-mass modification over Europe: EARLINET aerosol observations from Wales to Belarus. *J. Geophys. Res.*, 109, D24205.